Photosensitizer effect of 9-hydroxypheophorbide α on diode laser-irradiated laryngeal cancer cells: Oxidative stress-directed cell death and migration suppression

PEIJIE HE[1,2*], SHEN BO[3*], PHIL-SANG CHUNG[4], JIN-CHUL AHN[4] and LIANG ZHOU[1]

[1]Department of Otolaryngology-Head and Neck Surgery, Shanghai Key Clinical Disciplines of Otorhinolaryngology, Eye and ENT Hospital of Fudan University, Shanghai 200031; [2]Shanghai Public Health Clinical Center, Fudan University, Shanghai 201508; [3]Institute of Radiation Medicine, Fudan University, Shanghai 200032, P.R. China; [4]Department of Otolaryngology-Head and Neck Surgery, Medical Laser Research Center, College of Medicine, Dankook University, Cheonan 330-715, Republic of Korea

Abstract. The present study aimed to investigate the effect, and elucidate the potential mechanisms, of 9-hydroxypheophorbide α-based photodynamic therapy (9-HPbD-PDT) on apoptosis and necrosis induction, and migration suppression of laryngeal cancer AMC-HN-3 (HN-3) cells. Phototoxicity initiated by 9-HPbD-PDT on HN-3 cells was observed in a photosensitizer dose-dependent pattern. There was an initial increase of apoptotic cells coupled with gradual enhancement of reactive oxygen series (ROS) generation at lower doses of 9-HPbD. By contrast, at a higher dose of 9-HPbD, there was a clear increase of necrotic cells with a gradual decrease of ROS generation. Following PDT, an elevated percentage of apoptotic cells with shrinkage or condensing nuclei was observed using Hoechst 33342/propidium iodide double staining, and an upregulated expression of poly ADP-ribose polymerase was detected through western blotting. A disruption of the mitochondrial membrane potential was detected 2 h following PDT. Significant suppression of cell migration and downregulation of epidermal growth factor receptor (EGFR) expression were recorded following PDT. These results indicate that the distribution of photosensitizer leads to differences in the generation of ROS, which subsequently determines the type of cell death. Overall, mitochondrial activation under oxidative stress is important in the 9-HPbD-PDT-induced apoptosis of HN-3 cells. Migration suppression of HN-3 cells following PDT may be associated with the inhibited expression of EGFR, due to oxidative stress.

Introduction

As an emerging and promising cancer therapy, photodynamic therapy (PDT) activates and destroys photosensitizer-incubated tumor cells using wavelength-matched visible light irradiation. PDT initiates apoptotic and necrotic cell death *in vivo* and *in vitro* (1); however, the factors involved in the overall process and the contribution to either mechanism are not completely elucidated.

PDT has previously demonstrated novel effects in the treatment of oncologic diseases; however, the limitations of laser penetration into normal tissues and long-lasting cutaneous photosensitivity following irradiation are unavoidable, and may affect the applicability of PDT to malignant tumor therapy (2). As a novel chlorophyll derived photosensitizer, 9-hydroxypheophorbide α (9-HPbD) has a relatively longer absorption wavelength (664 nm) and a shorter half-life in the body compared with other photosentisizers (3). In addition, 9-HPbD exhibited an apoptosis-inducing effect and growth suppression in MCF-7 human breast cancer cells (3). A previous study concerning combination treatment with 9-HPbD-PDT and carboplatin resulted in an enhanced photocytotoxicity and apoptosis induction in laryngeal AMC-HN-3 (HN-3) cancer cells (4). Oxidative stress-directed cell death and migration suppression of HN-3 cells using 9-HPbD-PDT is additionally investigated in the present study.

The present study aimed to investigate the effect, and elucidate the potential mechanisms, of 9-HPbD-PDT on apoptosis and necrosis induction, as well as migration suppression, of HN-3 cells.

Materials and methods

Reagents and antibodies. All media and supplements for cell culture were supplied by Hyclone™ (GE Healthcare Life Sciences, Logan, UT, USA). Dimethyl sulfoxide (DMSO),

---

Correspondence to: Professor Liang Zhou or Dr Peijie He, Department of Otolaryngology-Head and Neck Surgery, Shanghai Key Clinical Disciplines of Otorhinolaryngology, Eye and ENT Hospital of Fudan University, 83 Fenyang Road, Shanghai 200031, P.R. China
E-mail: zhoulent@126.com
E-mail: hepj2002@sina.com

*Contributed equally

3-[4,5-dimethylthiazol-2-yl]-2,5-diphenyl-tetrazoliumbromide (MTT), RIPA buffer, protease [glutathione (GSH)] and phosphatase (ascorbic acid) inhibitors, Hoechst 33342 dye and propidium iodide (PI) were obtained from Sigma-Aldrich (St. Louis, MO, USA). 2',7'-dichlorodihydrofluorescein diacetate (H_2DCFDA; D399) and rhodamine 123 were purchased from Molecular Probes (Thermo Fisher Scientific, Inc., Waltham, MA, USA). Rabbit anti-GAPDH polyclonal antibody (cat. no. ab9485; dilution 1:2,000) was supplied by Abcam (Cambridge, UK); mouse anti-poly ADP-ribose polymerase (PARP) polyclonal antibody (cat. no. AM30; dilution 1:200) was obtained from Merck Millipore (Darmstadt, Germany); and goat anti-epidermal growth factor receptor (EGFR) polyclonal antibody (cat. no. sc-03-G; dilution 1:200) was purchased from Santa Cruz Biotechnology, Inc. (Dallas, TX, USA).

Cell culture. The HN-3 cell line (5) was developed from a 63-year-male patient with previously untreated laryngeal squamous cell carcinoma, and was kindly provided by Asan Medical Center (Seoul, Korea). The cell line was cultured in RPMI-1640 medium supplemented with 10% fetal bovine serum, penicillin (50 units/ml) and streptomycin (50 μg/ml) at 37°C in a 5% CO_2 and 95% air atmosphere in a humidified incubator.

PDT protocol. 9-HPbD (3) was kindly donated by Kumho Life and Environmental Science Laboratory (Kwangju, Korea). 9-HPbD was stored in ethanol (1.5 mg/ml) and aluminum foil at -20°C. HN-3 cells at 90% confluence were incubated with 9-HPbD in the dark for 6 h at 37°C. Subsequent to changing the culture medium, 9-HPbD-photosensitized cells were subsequently exposed to a 664 nm diode laser (Hi-Tech Optoelectronics, Co., Ltd., Beijing, China) at 2.0 J/cm² for 15 min. In order to assess the antioxidant effect, HN-3 cells were incubated simultaneously with either 5 mM GSH or 2.5 mM ascorbic acid and 0.59 μg/ml 9-HPbD. Subsequently, the incubated cells were irradiated by laser, according to the aforementioned conditions.

Cell viability assay. A MTT assay was used to measure cell viability. The treated cells at 90% confluence were incubated with 50 μl MTT solution (2 mg/ml) for 2 h. The MTT solution was exchanged with 100 μl DMSO and the absorbance at 540 nm was measured following 20 sec of shaking. Cell viability was calculated according to the following equation: Cell viability (%) = (mean absorbance in treatment group / mean absorbance in control group) x 100.

Detection of reactive oxygen species (ROS) and 9-HPbD fluorescence. Generation of ROS was detected by H_2DCFDA staining as previously described (6). In brief, treated cells at 90% confluence were incubated with 2 μM H_2DCFDA at 37°C for 30 min, and then gently washed twice with Dulbecco's phosphate-buffered saline (DPBS). Images of green H_2DCFDA were captured using an excitation light from a 488 nm argon laser, 560 nm dichroic mirror and 505-550 nm band pass barrier filter. 9-HPbD was excited with a 633 nm helium/neon laser. Band-pass emission filters of 530-600 and 420-480 nm were used to identify ROS green signal (channel 1) and 9-HPbD red

fluorescence (channel 2). A 650 nm long pass emission filter was applied for 9-HPbD.

Hoechst 33342 and PI double staining. The treated cells at 90% confluence were stained with Hoechst 33342 for 30 min and PI for 10 min and observed using confocal microscopy, as previously described (4). Hoechst 33342 is a fluorescent dye that specifically stains nucleic acid. Hoechst 33342-stained normal cells exhibit regular and round nuclei (blue), while the nuclei of apoptotic cells are crimpy or condensed (bright blue). However, PI penetrates the cytoplasmic membrane of oncotic cells (late apoptotic and necrotic cells) and stains the nuclei pink. Due to the intact cytoplasmic membrane, the nuclei of normal cells and early apoptotic cells are not stained by PI.

Measurement of mitochondrial membrane potential (MMP). In brief, the treated cells at 60-70% confluence were stained with 1 μM rhodamine 123 for 30 min, and subsequently the cells were gently washed twice with DPBS. Images of green fluorescence from rhodamine 123 stained mitochondria were captured with confocal microscopy with an excitation wavelength of 488 nm, 560 nm dichroic mirror and 505-550 nm band pass barrier filter. MMP was further detected using flow cytometry (BD Biosciences, San Jose, CA, USA). Briefly, suspended cells were incubated with 1 μM rhodamine 123 for 30 min and monitored by the FL1-H channel. Data were analyzed using BD CellQuest™ Pro software, version 2.0 (BD Biosciences). A minimum of 20,000 events were counted.

Wound healing assay. The HN-3 cells were cultured in 10 cm petri dishes until the monolayer was 80-90% confluent. Following PDT treatment, the cell monolayer was lesioned using a 1.2 mm cell scraper without damaging the dish surface. Images of the lesion areas were captured at 0 and 24 h following PDT. The photos were analyzed using Adobe Photoshop CS6 (Adobe Systems Inc., San Jose, CA, USA). The distance of cell migration was calculated by subtracting the distance between the lesion edges at 24 h from the distance measured at 0 h. The values were expressed in mm.

Western blotting analysis. Following treatment with PDT, the cells at 90% confluence were harvested and total proteins were extracted using RIPA buffer. Protein concentrations were determined with Bradford dye reagent. Equivalent amounts of protein (100 μg) were loaded onto 10% polyacrylamide gels, subjected to electrophoresis, and transferred to polyvinylidene difluoride membranes. Electrophoresis and blotting were performed using the PowerPac™ Basic Power Supply Electrophoresis System 200 (Bio-Rad Laboratories, Inc., Hercules, CA, USA). The membranes were blocked with 5% skimmed milk for 1 h, followed by incubation with the primary antibodies against PARP, EGFR and GAPDH overnight at 4°C. Subsequently, the membranes were incubated with horseradish peroxidase-conjugated goat anti-mouse IgG (cat. no. sc-2005; dilution 1:2,000; Santa Cruz Biotechnology, Inc.), goat anti-rabbit IgG (cat. no. sc-2004; dilution 1:2000; Santa Cruz Biotechnology, Inc.) or mouse anti-goat IgG (cat. no. sc-2355; dilution 1:2,000; Santa Cruz Biotechnology, Inc.) for 1 h. The protein bands were detected by
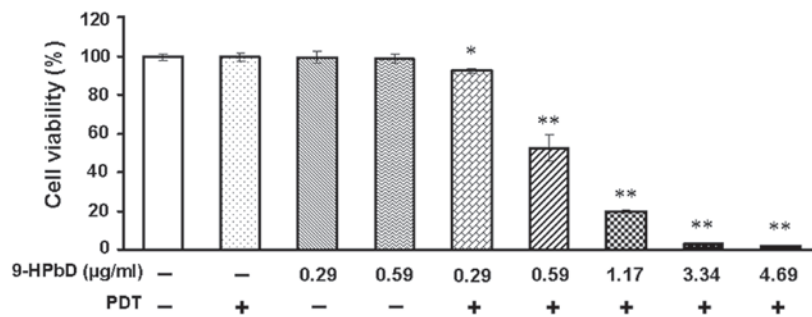
Figure 1. Cytotoxicity of 9-HPbD-mediated PDT on laryngeal cancer AMC-HN-3 cells. A MTT assay was performed to assess cell viability 24 h following PDT. Data are presented as the mean ± standard deviation of three independent experiments. *P<0.05, **P<0.01 vs. control cells. PDT, photodynamic therapy; HPbD, 9-hydroxypheophorbide α.

a Kodak *in vivo* Image Analyzer (Kodak, Rochester, NY, USA).

Statistical analysis. Results are expressed as the mean ± standard deviation. Significant differences were evaluated using one-way analysis of variance followed by least significant difference method. Statistical analyses were performed using SPSS 11.5 software (SPSS, Inc., Chicago, IL, USA). P<0.05 was considered to indicate a statistically significant difference.

Results

Photocytotoxic effect of 9-HPbD. The photocytotoxicity exhibited by 9-HPbD-PDT on HN-3 cells was validated by a MTT assay. With diode laser irradiation, the photocytotoxic effect of 9-HPbD on HN-3 cells exhibited a photosensitizer dose-dependent pattern. Neither PDT nor 9-HPbD alone was photocytotoxic to HN-3 cells. As shown in Fig. 1, cell viability was significantly suppressed at 0.29 μg/ml 9-HPbD-PDT compared with control cells (P=0.021). At higher doses of 9-HPbD (≥0.59 μg/ml), cell viability was also significantly suppressed compared with control cells (P<0.01).

ROS generation, 9-HPbD fluorescence and cell death induction by 9-HPbD-PDT. As shown in Fig. 2A, 9-HPbD fluorescence was increased with increasing doses of 9-HPbD. Intracellular formation of ROS was detected by the conversion of non-fluorescent H_2DCFDA to fluorescent 2,7-dichlorofluorescein diacetate (DCFDA). As shown in Fig. 2A, DCFDA fluorescence increased between 0.29 and 1.17 μg/ml 9-HPbD-PDT. Subsequently, the intensity of DCFDA fluorescence broke down gradually between 1.17 and 4.69 μg/ml 9-HPbD-PDT 1 h following laser irradiation.

A total of 24 h following PDT, the cells exhibited blurred and shrinkable cellular contours. Apoptotic cells, marked with condensed/fragmented blue or pink nuclei, were observed in a dose-dependent manner following treatment with 0.29-1.17 μg/ml 9-HPbD-PDT. There was a gradual increase in necrotic cells, which exhibited pink intact nuclei, in cells treated with higher doses of 9-HPbD (1.17-4.69 μg/ml). The cells in the control group exhibited intact homogeneous blue and round nuclei (Fig. 2B). Apoptotic/necrotic cells were not observed in cells treated with 9-HPbD or laser irradiation alone (data not shown).

9-HPbD-PDT initiates mitochondrial depolarization. Cells were stained with rhodamine 123, and MMP in single cells was monitored using flow cytometry and confocal microscopy. A collapsed MMP, shown as a leftward shift of the fluorescence curve from flow cytometry, was observed in a 9-HPbD dose-dependent manner (Fig. 3A). Polarized mitochondria were demonstrated by the presence of bright fluorescent spheres and tubes using confocal microscopy. A total of 2 h following PDT, the majority of the bright spheres became faint and rhodamine 123 fluorescence intensity was caliginous, indicating mitochondrial depolarization (Fig. 3B).

9-HPbD-PDT suppressed the migration and EGFR expression in HN-3 cells. A wound healing assay was used to evaluate the effect of 9-HPbD-PDT on the migration of HN-3 cells. As shown in Fig. 4, PDT significantly suppressed the migration of HN-3 cells in a sensitizer dose-dependent manner. The migration distance of HN-3 cells decreased from 0.74±0.07 observed in the control group to 0.63±0.07 mm in the 0.29 μg/ml 9-HPbD-PDT group (P=0.007) and 0.13±0.05 mm in the 0.59 μg/ml 9-HPbD-PDT group (P=0.001) (Fig. 4).

In contrast to the untreated group, there was clear inhibition of EGFR expression in PDT groups in a sensitizer dose-dependent manner (Fig. 5A). Downregulation in the expression of EGFR was partially inhibited when the cells were pretreated with ascorbic acid (Fig. 5B). As the native substrate of caspase-3, PARP was measured using western blotting. Similarly to EGFR expression, there was an elevated expression of PARP in a sensitizer dose-dependent manner (Fig. 5A). When cells were pretreated with GSH and ascorbic acid, upregulation of PARP was significantly inhibited (Fig. 5B).

Discussion

In the present study, phototoxicity was not observed when HN-3 cells were treated with 9-HPbD or laser irradiation alone. In the presence of a laser, 9-HPbD had significant photocytotoxicity and an induction of apoptosis and necrosis was observed, which was a photosensitizer dose-dependent response. These results demonstrate the basic rule of PDT: There is a synergistic effect between lasers and photosensitizers, which is required since laser nor photosensitizer alone is photocytotoxic (7).

The basic principle of PDT is that rapid ROS generation, due to the photochemical activation of the photosensitizer, initiates cell death (8). Consistent with increased ROS signals,
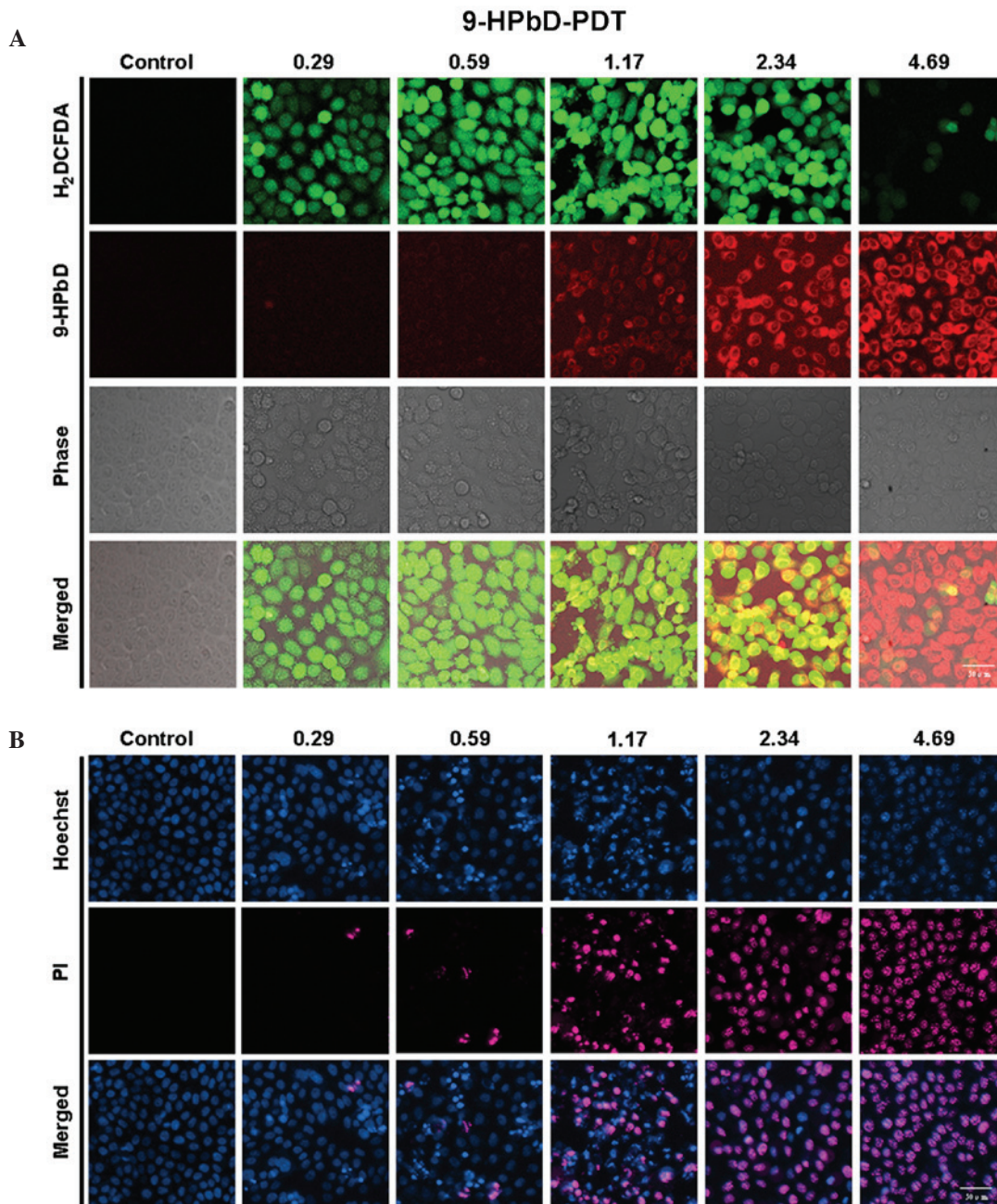
Figure 2. Accumulation of ROS and 9-HPbD fluorescence, and apoptosis and necrosis of laryngeal cancer AMC-HN-3 cells was observed following PDT under a laser scanning confocal microscope. (A) ROS were measured 1 h following PDT and the fluorescence signal of 9-HPbD was captured simultaneously. (B) Representative fluorescent microscopic images of Hoechst 33342 and PI staining were obtained 24 h following PDT. Scale bar, 20 µm. ROS, reactive oxygen species; 9-HPbD, 9-hydroxypheophorbide α; PDT, photodynamic therapy; H$_2$DCFDA, 2',7'-dichlorodihydrofluorescein diacetate; PI, propidium iodide.

in the present study there was gradually induction of apoptosis in HN-3 cells treated with 0.29-1.17 µg/ml 9-HPbD-PDT. In cells treated with higher doses of 9-HPbD-PDT (1.17-4.69 µg/ml), there was a gradual increase of necrotic cells with 9-HPbD concentration, whereas ROS signals were remarkably attenuated. This may be associated with nonspecific relocalization of photosensitizer targets at higher doses, including to lysosomes or the plasma membrane, which may either block or delay the apoptotic program, thus predisposing the cells to necrosis (9). Apoptotic and necrotic cells were not observed when cells were treated with 9-HPbD or a laser alone (data not shown). These results suggest that 9-HPbD shares the same characteristics as other photosensitizers;

photosensitizers minimize the undesirable effects of anti-tumor drugs towards normal tissue during treatment (2). This is one of the advantages of PDT over other conventional cancer treatment modalities, including surgery, radiation and chemotherapy. The advantage of selective tumor destruction with normal tissue preservation is of particular importance for cancers in the head and neck region, where excessive tissue loss results in significant functional disabilities including effects on speech and swallowing (2,10).

A positive regulatory function of PARP cleavage has been observed in the onset of apoptosis (11). PARP, the native substrate of caspase-3 (12), was measured in the present study by western blotting, and this revealed that PARP was
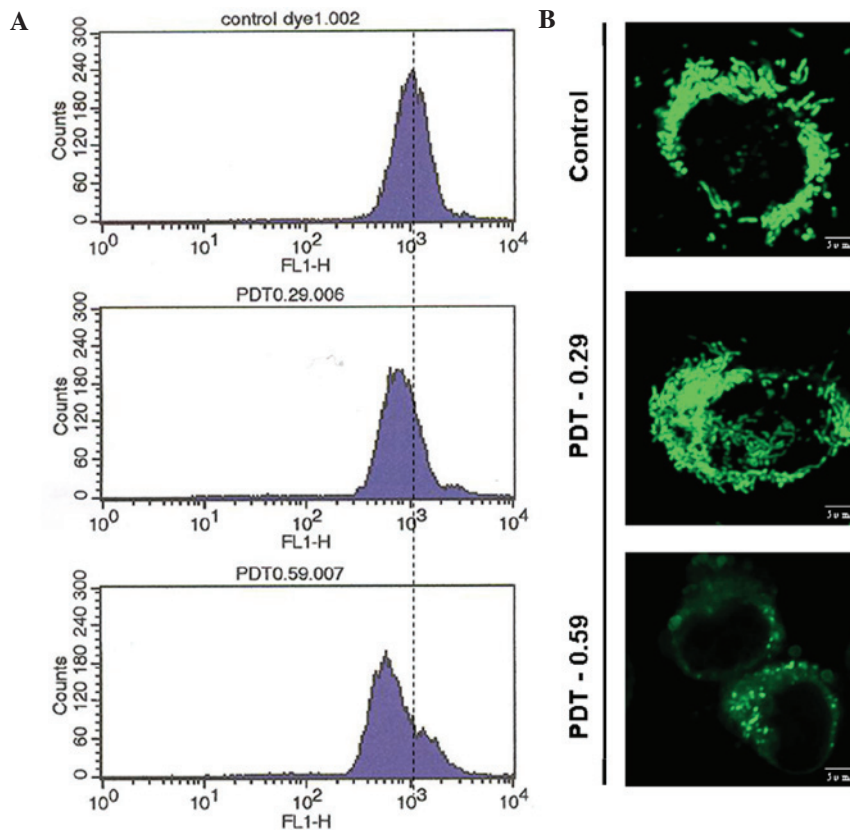
Figure 3. 9-hydroxypheophorbide α-PDT induced MMP collapse of laryngeal cancer AMC-HN-3 cells. MMP was detected 2 h following PDT using (A) flow cytometry and (B) confocal microscopy. (A) The distribution of MMP was shown as a blue-shaded area. Baseline MMP in the control group was labeled as a broken line. The spectral shift of the blue-shaded area to the left indicates mitochondrial membrane depolarization. A representative experiment of three repeats is presented. (B) Images of green fluorescence from rhodamine 123 stained mitochondria were captured by confocal microscopy (scale bar, 5 μm). PDT, photodynamic therapy; MMP, mitochondrial membrane potential.
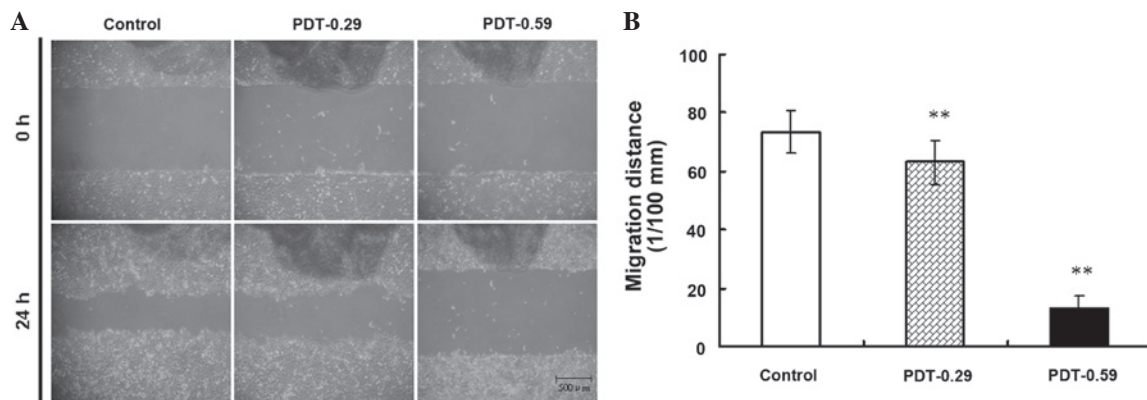

Figure 4. 9-hydroxypheophorbide α-PDT suppressed cell migration in a wound healing assay. (A) Monolayer of laryngeal cancer AMC-HN-3 cells were lesioned by a scraper in a petri dish. Repair of the lesion by cell migration following PDT was photographed 24 h later. (B) Total migrating distance of AMC-HN-3 cells from the edges of the lesion was measured 24 h following PDT. Data are presented as the mean ± standard deviation from three independent experiments. **P<0.01 vs. control. Scale bar, 500 μm. PDT, photodynamic therapy.

upregulated 24 h following PDT. The increased expression of cleaved PARP, consistent with an enhanced cytotoxic and apoptotic effect of PDT, was significantly inhibited by antioxidant pretreatment, including GSH and ascorbic acid. The pattern of PARP expression under oxidative stress further indicates the role of ROS in 9-HPbD-PDT-induced apoptosis.

Although the involvement of multiple pathways during PDT-mediated cell death has been reported (1), the elucidation of the molecular mechanisms underlying PDT-mediated apoptosis and cell cycle deregulation is far from complete. An improved understanding of these pathways may lead to development of strategies for improving treatment proto-cols (4,13,14), and therefore, increase the therapeutic efficacy of PDT.

Mitochondria are recognized as the most important cellular organelle for apoptosis inducement (15,16). Generally,
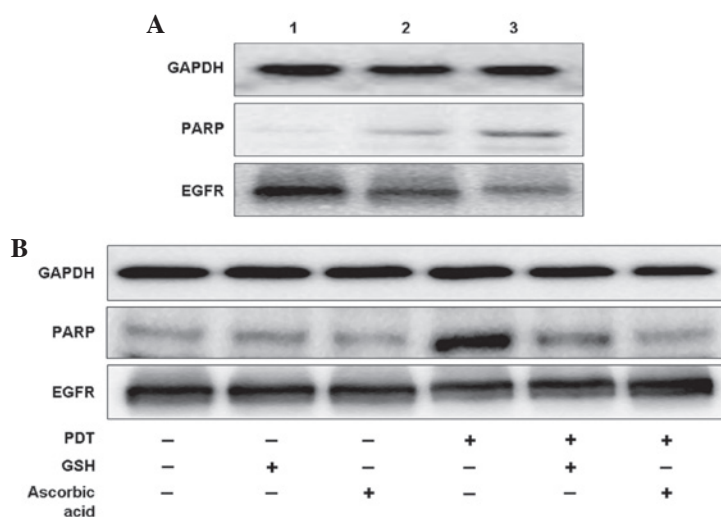
Figure 5. 9-HPbD-PDT induced the cleavage of PARP (89 kDa), and inhibited the expression of EGFR (170 kDa). Laryngeal cancer AMC-HN-3 cells were treated with a sublethal dose of PDT, collected 24 h later, and subjected to western blot analysis. GAPDH (37 kDa) was used as a control. (A) Lane 1, control (no treatment); lane 2, 0.29 µg/ml 9-HPbD-PDT; lane 3, 0.59 µg/ml 9-HPbD-PDT. (B) Cells were treated with 0.59 µg/ml 9-HPbD-PDT alone or pretreated with 5 mM GSH or 2.5 mM ascorbic acid. GAPDH, glyceraldehyde 3-phosphate dehydrogenase; PARP, poly ADP-ribose polymerase; EGFR, epidermal growth factor receptor; 9-HpbD, 9-hydroxypheophorbide α; PDT, photodynamic therapy; GSH, glutathione.

prior to cell death, a collapse of MMP is initiated. Collapsed MMP has been considered as an important factor that initiates the release of cytochrome *c* (17). Following the release of mitochondrial cytochrome *c* into the cytosol, activation of the caspase cascade has been reported in PDT-induced apoptosis (18). In the present study, a clear leftward shift of the fluorescence curve indicated a collapse of MMP in HN-3 cells treated with 9-HPbD-PDT, which occurred in a photosensitizer dose-dependent pattern. Similarly with increasing doses of 9-HPbD, mitochondrial morphology exhibited a gradual loss of characteristically bright spheres/tubes and more diffuse and weaker fluorescent signals were observed following PDT, due to leakage of the dye from the mitochondria into the cytosol. The disruption of MMP demonstrates the important role of mitochondria activation of apoptosis in HN-3 cells treated with 9-HPbD-PDT.

An increased expression of EGFR has been reported in 90% of squamous cancer cells in the head and neck region (19). It has been indicated that EGFR is important in tumor progression, in addition to its role in cellular proliferation (20); therefore, EGFR-inhibition has been recently considered as a candidate for the treatment of head and neck carcinoma (21,22). In the present study, there was a significant downregulation in the expression of EGFR in PDT groups in a photosensitizer dose-dependent manner compared with the high expression of EGFR observed in the control group, which may subsequently lead to migration suppression of HN-3 cancer cells, as observed in a previous experiment. This indicates that EGFR may be the target of 9-HPbD-PDT in HN-3 cells. EGFR also has a role in the activation of cell apoptosis and necrosis (23). A downregulated expression of EGFR following PDT was partially inhibited by pretreatment with ascorbic acid, indicating a potential role of ROS in 9-HPbD-PDT-induced migration suppression.

Overall, 9-HPbD-PDT exhibits a phototoxic effect in HN-3 cells, as evidenced by an attenuated cell viability and activation of apoptosis and necrosis observed by the present study.

Mitochondrial activation under oxidative stress is important in 9-HPbD-PDT-induced apoptosis of HN-3 cells. The subcellular relocalization of 9-HPbD may lead to the distinguishing generation of ROS and subsequently determine the type of cell death. Migration suppression of HN-3 cells following PDT is partially due to the ROS-mediated inhibition of EGFR expression and/or phosphorylation (23). However, the potential mechanisms involved in the photochemical effect of 9-HPbD-PDT on HN-3 cancer cells require further investigation.

Acknowledgements

References

1. Buytaert E, Dewaele M and Agostinis P: Molecular effectors of multiple cell death pathways initiated by photodynamic therapy. Biochim Biophys Acta 1776: 86-107, 2007.
2. Agostinis P, Berg K, Cengel KA, Foster TH, Girotti AW, Gollnick SO, Hahn SM, Hamblin MR, Juzeniene A, Kessel D, *et al*: Photodynamic therapy of cancer: An update. CA Cancer J Clin 61: 250-281, 2011.
3. Choi SE, Sohn S, Cho JW, Shin EA, Song PS and Kang Y: 9-Hydroxypheophorbide α-induced apoptotic death of MCF-7 breast cancer cells is mediated by c-Jun N-terminal kinase activation. J Photochem Photobiol B 73: 101-107, 2004.
4. He P, Ahn JC, Shin JI, Hwang HJ, Kang JW, Lee SJ and Chung PS: Enhanced apoptotic effect of combined modality of 9-hydroxypheophorbide alpha-mediated photodynamic therapy and carboplatin on AMC-HN-3 human head and neck cancer cells. Oncol Rep 21: 329-334, 2009.

5. Kim SY, Chu KC, Lee HR, Lee KS and Carey TE: Establishment and characterization of nine new head and neck cancer cell lines. Acta Otolaryngol 117: 775-784, 1997.
6. Chung PS, He P, Shin JI, Hwang HJ, Lee SJ and Ahn JC: Photodynamic therapy with 9-hydroxypheophorbide alpha on AMC-HN-3 human head and neck cancer cells: Induction of apoptosis via photo-activation of mitochondria and endoplasmic reticulum. Cancer Biol Ther 8: 1343-1351, 2009.
7. Moan J and Berg K: Photochemotherapy of cancer: Experimental research. Photochem Photobiol 55: 931-948, 1992.
8. Moan J and Berg K: The photodegradation of porphyrins in cells can be used to estimate the lifetime of singlet oxygen. Photochem Photobiol 53: 549-553, 1991.
9. Oleinick NL, Morris RL and Belichenko I: The role of apoptosis in response to photodynamic therapy: What, where, why, and how. Photochem Photobiol Sci 1: 1-21, 2002.
10. Biel MA: Photodynamic therapy treatment of early oral and laryngeal cancers. Photochem Photobiol 83: 1063-1068, 2007.
11. Boulares AH, Yakovlev AG, Ivanova V, Stoica BA, Wang G, Iyer S and Smulson M: Role of poly (ADP-ribose) polymerase (PARP) cleavage in apoptosis: Caspase 3-resistant PARP mutant increases rates of apoptosis in transfected cells. J Biol Chem 274: 22932-22940, 1999.
12. Tewari M, Quan LT, O'Rourke K, Desnoyers S, Zeng Z, Beidler DR, Poirier GG, Salvesen GS and Dixit VM: Yama/CPP32 beta, a mammalian homolog of CED-3, is a CrmA-inhibitable protease that cleaves the death substrate poly(ADP-ribose) polymerase. Cell 81: 801-809, 1995.
13. Verma S, Watt GM, Mai Z and Hasan T: Strategies for enhanced photodynamic therapy effects. Photochem Photobiol 83: 996-1005, 2007.
14. Fang X, Wu P, Li J, Qi L, Tang Y, Jiang W and Zhao S: Combination of apoptin with photodynamic therapy induces nasopharyngeal carcinoma cell death in vitro and in vivo. Oncol Rep 28: 2077-2082, 2012.
15. Liu JX, Zhang JH, Li HH, Lai FJ, Chen KJ, Chen H, Luo J, Guo HC, Wang ZH and Lin SZ: Emodin induces Panc-1 cell apoptosis via declining the mitochondrial membrane potential. Oncol Rep 28: 1991-1996, 2012.
16. Wang CZ, Calway TD, Wen XD, Smith J, Yu C, Wang Y, Mehendale SR and Yuan CS: Hydrophobic flavonoids from Scutellaria baicalensis induce colorectal cancer cell apoptosis through a mitochondrial-mediated pathway. Int J Oncol 42: 1018-1026, 2013.
17. Lai JC, Lo PC, Ng DK, Ko WH, Leung SC, Fung KP and Fong WP: BAM-SiPc, a novel agent for photodynamic therapy, induces apoptosis in human hepatocarcinoma HepG2 cells by a direct mitochondrial action. Cancer Biol Ther 5: 413-418, 2006.
18. Granville DJ, Shaw JR, Leong S, Carthy CM, Margaron P, Hunt DW and McManus BM: Release of cytochrome c, Bax migration, Bid cleavage, and activation of caspases 2, 3, 6, 7, 8 and 9 during endothelial cell apoptosis. Am J Pathol 155: 1021-1025, 1999.
19. Kalyankrishna S and Grandis JR: Epidermal growth factor receptor biology in head and neck cancer. J Clin Oncol 24: 2666-2672, 2006.
20. Woodburn JR: The epidermal growth factor receptor and its inhibition in cancer therapy. Pharmacol Ther 82: 241-250, 1999.
21. Kim SG, Hong JW, Boo SH, Kim MG, Lee KD, Ahn JC, Hwang HJ, Shin JI, Lee SJ, Oh JK and Chung PS: Combination treatment of Cetuximab and photodynamic therapy in SNU-1041 squamous cancer cell line. Oncol Rep 22: 701-708, 2009.
22. Koon HK, Chan PS, Wong RN, Wu ZG, Lung ML, Chang CK and Mak NK: Targeted inhibition of the EGFR pathways enhances Zn-BC-AM PDT-induced apoptosis in well-differentiated nasopharyngeal carcinoma cells. J Cell Biochem 108: 1356-1363, 2009.
23. Martínez-Carpio PA and Trelles MA: The role of epidermal growth factor receptor in photodynamic therapy: A review of the literature and proposal for future investigation. Lasers Med Sci 25: 767-771, 2010.